Strojniški vestnik - Journal of Mechanical Engineering 64(2018)10, 601-610
DOI:10.5545/sv-jme.2018.5242
Original Scientific Paper
Received for review: 2018-01-26
Received revised form: 2018-05-31
Accepted for publication: 2018-06-13

Research of Crack Detection and Delay Crack Propagation on a Nonlinear Rotor

Jun Liu[1,2,*] – Weilong Liu[1] – Xiaofeng Wang[1,2]

[1] Tianjin Key Laboratory of the Design and Intelligent Control of the Advanced Mechanical System, China
[2] National Demonstration Center for Experimental Mechanical and Electrical Engineering Education, China

The existence and propagation of a crack on an engine's nonlinear rotor can easily cause a serious accident, so it is quite essential to detect a crack in the rotor system through analysis of the rotor's vibration signals and to delay the crack propagation. The vibration signals of the cracked rotor show the non-periodic and the nonlinearity within a transient response. The fault characteristics of the crack can be easily hidden in other vibrational components and are difficult to extract from transient signals. In the paper, the Hilbert-Huang marginal spectrum (HHMS) method is proposed to realize the extraction of crack's fault characteristics in a nonlinear rotor system. In addition, the crack's opening and closing degrees at any rotating position are also put forward representing the crack propagation, and some tactics of the delaying crack propagation are proposed based on the effect on the crack's opening and closing degree caused by the change of different rotor parameters. The simulation results show that the HHMS method can detect a crack early at about five per cent of the depth of the rotor's diameter, and the methods of delaying crack propagation can effectively delay propagation. Experimental results verify the effectiveness of the proposed HHMS method.

Keywords: cracked rotor, transient response, Hilbert-Huang marginal spectrum, crack detection, delaying crack propagation

Highlights

- *The crack fault can be effectively extracted by the HHMS method from complex vibration signals.*
- *The effectiveness of the proposed HHMS method was verified by the experimental and simulation results.*
- *Increasing the rotational acceleration can delay the crack propagation.*
- *When the angle β and the support of the rotor are adjusted effectively, the delay crack propagation can be achieved, such as reducing the symmetric nonlinear term $\beta^{(0)}$ and increasing the value of the asymmetric nonlinear term $\varepsilon_c^{(1)}$ and $\varepsilon_s^{(1)}$.*

0 INTRODUCTION

Engines are essential to the aircraft, and the rotor system is the key component of the engine. The rotor system usually works in difficult environments with multiple coupling fields, which include high temperatures, high pressures, high loads, and periodic alternating loads. Such an environment makes the rotor system generate micro-cracks and micro-defects, and the defects could cause severe accidents when the crack propagates. In recent decades, researchers have identified cracks through the analysis of vibration signals of a rotor system, and this research has supplied some significant achievements. The Fourier transform **[1]** and **[2]** can be used to transfer the periodic signal from the time domain to the frequency domain, and engineers use the frequency characteristics of the detected signals to analyze any faults. However, it is only able to deal with periodic signals and can not process non-periodic signals. The short-time Fourier transform (STFT) **[3]** and **[4]** can obtain the time-varying spectrum of the detected signal by imposing a time window on the detected signal and then sliding the time window to do the Fourier transform with data of the time window. However, a contradiction of the time domain resolution and frequency domain resolution exists; therefore, the resolution accuracy could be affected. The Winger-Ville distribution **[5]** and **[6]** has a good time-frequency clustering, and it is a quadratic time-frequency method. When it is used to analyse the multi-component signals **[7]**, it will produce serious cross-item interference and a false frequency that does not exist in the actual signal. The wavelet transform **[8]** and **[9]** can express local characteristics in the time-frequency domain. Because it needs to select different parameters of the wavelet function according to different detected signals, the analysis results depend heavily on the selecting parameters of the wavelet function. The Hilbert-Huang transform (HHT) **[10]** and **[11]** is a novel signal analysis method on the time-frequency domain, and the marginal spectrum of the signal can be obtained by integrating the Hilbert spectrum **[12]** to **[14]**, which can accurately reflect the change of the signal amplitude on the frequency domain. The HHT has already been applied to voice recognition, bearing fault detection, and other fields.

An aircraft's engine's rotor often works under the transient conditions when the aircraft takes off or lands, performs stunts, or follows a climbing-diving flight model **[15]**. The vibration signal of the cracked rotor system exhibits the non-periodic and nonlinear

*Corr. Author's Address: Tianjin University of Technology, No. 391 Binshuixi Road, Tianjin 300384, China, liujunjp@tjut.edu.cn

transitional characteristics under the transient response, and a weak fault characteristic is easily hidden in other transition components.

Based on the above problems, the HHMS method is proposed to realize the extraction of the crack's fault on a cracked rotor. The simulation results show that the proposed method can effectively extract the crack's fault characteristics, and it can overcome above the faults of other methods. Based on the novel model of the crack's opening and closing, which can flexibly describe the crack's opening and closing degree of the rotor at any rotational position, the strategy of delaying crack propagation is discussed by analysing the crack's opening and closing degree with different rotors' parameters. Experimental results have also verified the effectiveness of the HHMS method.

1 MODEL DESCRIPTION

1.1 Rotor Model

The Jeffcott rotor model with a lateral crack is shown in Fig. 1, and the disc is mounted on the centre of the elastic symmetrical shaft with a certain eccentric mass, and the crack is close to the disc. The horizontal rotor is supported at one end by a double-row of self-aligning ball bearing and at the other end by a single-row of deep-groove ball bearing. Because the single-row of deep-groove ball-bearing radial tilts have some rotational constraints, the elastic restoring force to be applied to the rotor will show nonlinearities, and the vibrations of the rotor will also appear to have nonlinear vibration characteristics. The differential equations of motion of the nonlinear rotor system under the transient response are shown below.

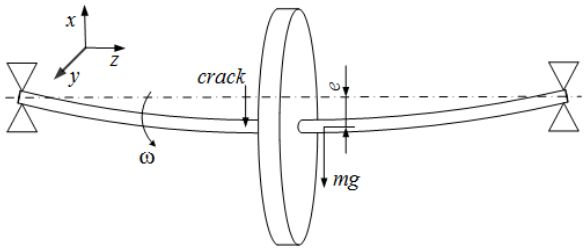

Fig. 1. *Jeffcott rotor model with a lateral crack*

$$\begin{cases} m\ddot{x}+c\dot{x}+kx+N_x = me\omega^2\cos(\omega_0 t+\frac{1}{2}\lambda t^2+\phi_0) \\ +me\lambda\sin(\omega_0 t+\frac{1}{2}\lambda t^2+\phi_0)+mg \\ m\ddot{y}+c\dot{y}+ky+N_y = me\omega^2\sin(\omega_0 t+\frac{1}{2}\lambda t^2+\phi_0) \\ +me\lambda\cos(\omega_0 t+\frac{1}{2}\lambda t^2+\phi_0) \end{cases}, \quad (1)$$

where m is the disc mass, c is the damping coefficient, k is the stiffness coefficient, ω is the rotational speed, λ is the rotational acceleration, and e is the static unbalance of the disk. N_x and N_y are the nonlinear elastic restoring forces [16], corresponding to the x- and y-directions of the nonlinear term, respectively.

1.2 Stiffness Model of Cracked Rotor

The relationship among the parameters is shown in Fig. 2. Due to the presence of the crack breath behaviour in a cracked rotor system, the rotor stiffness is changed during per revolution cycle. The stiffness model obtained by the neutral axis theory can accurately describe the crack's opening and closing process [17] and [18], and the mathematical equation [19] of the stiffness of the crack direction is shown as follows.

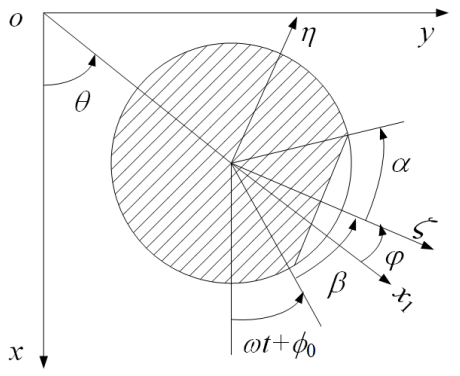

Fig. 2. *Schematic diagram of coordinate and parameter of a cracked rotor*

$$k_\varsigma(\alpha,\varphi)/k=\begin{cases}1-\dfrac{\alpha}{\pi}+\dfrac{\sin(4\alpha)}{4\pi}, & -\dfrac{\pi}{2}+\alpha\le\varphi<\dfrac{\pi}{2}-\alpha\\ \dfrac{3}{4}-\dfrac{\alpha}{2\pi}+\dfrac{\sin(4\alpha)}{8\pi}+\dfrac{\varphi}{2\pi}-\dfrac{\sin(4\pi)}{8\pi}+\dfrac{\cot\varphi}{\pi}(\cos^4\alpha-\sin^4\varphi), & \dfrac{\pi}{2}-\alpha\le\varphi<\dfrac{\pi}{2}+\alpha\\ 1, & \dfrac{\pi}{2}+\alpha\le\varphi<\dfrac{3\pi}{2}-\alpha\\ \dfrac{7}{4}-\dfrac{\alpha}{2\pi}+\dfrac{\sin(4\alpha)}{8\pi}-\dfrac{\varphi}{2\pi}+\dfrac{\sin(4\varphi)}{8\pi}-\dfrac{\cot\varphi}{\pi}(\cos^4\alpha-\sin^4\varphi), & \dfrac{3\pi}{2}-\alpha\le\varphi<\dfrac{3\pi}{2}+\alpha\end{cases}. \quad (2)$$

There is the relationship of $\varphi=\omega t+\phi_0+\beta-\theta$ and α is one-half angle of the crack. The stiffness on the rotational coordinate system is converted to the fixed coordinate system; the stiffness equations are shown following.

$$\begin{cases}k_x=k_\varsigma\cos^2(\omega t)+k_\eta\sin^2(\omega t)-k_{\varsigma\eta}\sin(2\omega t)\\ k_y=k_\varsigma\sin^2(\omega t)+k_\eta\cos^2(\omega t)+k_{\varsigma\eta}\sin(2\omega t)\\ k_{xy}=(k_\varsigma-k_\eta)\sin(\omega t)\cos(\omega t)+k_{\varsigma\eta}\cos(2\omega t)\end{cases}. \quad (3)$$

For convenient calculation, the transformation variables of the dimensionless parameters are shown as follows, and the dimensionless equations of the nonlinear cracked rotor can be obtained by using the transformation variables.

$$\delta=mg/k,\quad \bar{x}=x/\delta,\quad \bar{y}=y/\delta,\quad \bar{e}=e/\delta,$$
$$\omega_n=\sqrt{k/m},\quad \bar{t}=\omega_n t,\quad \bar{c}=c/(m\omega_n),\quad \bar{k}_x=k_x/k,$$
$$\bar{k}_y=k_y/k,\quad \bar{k}_{xy}=k_{xy}/k,\quad \bar{\lambda}=\lambda/\omega_n^2.$$

For simplicity, the dimensionless variables superscript'-'are eliminated. The dimensionless equations of the cracked rotor system are shown as follows.

$$\begin{cases}\ddot{x}+c\dot{x}+k_x x+k_{xy}y+N_x=1+\\ e\omega^2\cos(\omega_0 t+\dfrac{1}{2}\lambda t^2+\phi_0)+e\lambda\sin(\omega_0 t+\dfrac{1}{2}\lambda t^2+\phi_0)\\ \ddot{y}+c\dot{y}+k_y y+k_{xy}x+N_y=e\omega^2\sin(\omega_0 t+\dfrac{1}{2}\lambda t^2+\phi_0)\\ +e\lambda\cos(\omega_0 t+\dfrac{1}{2}\lambda t^2+\phi_0)\end{cases}. \quad (4)$$

1.3 Model of Crack's Opening and Closing Degree

In the reference [20], a model for describing the crack opening and closing degree is proposed to indirectly reflect crack propagation. However, it can only express the special state in which the rotor's crack is located in a fully opened state, shown in Fig. 3. In this paper, the mathematic stiffness model of the crack's opening and closing degree for the rotor at any rotational position can be described by combining the improved mathematical expression.

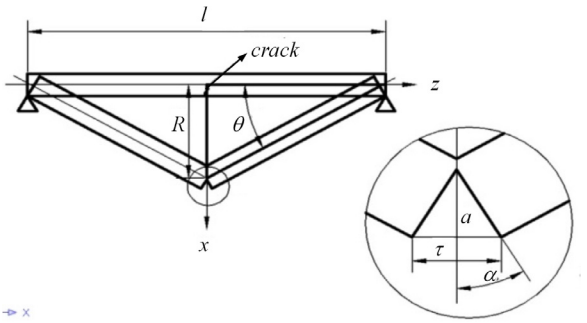

Fig. 3. *Model of crack's opening and closing degree*

When ζ coincides with x_1 shown in Fig. 2, the cracked position is shown in Fig. 3. The mathematical model of the crack's opening and closing degree is shown as follows.

$$\tau=4aR/\sqrt{l^2+4R^2}, \quad (5)$$

where R expresses the computational result of $R=\sqrt{x^2+y^2}$, a is the depth of a crack and l is the length of a rotor.

At this time, the corresponding value φ is equal to 0, and the crack's opening and closing degree locates the maximum value. When the angle φ is equal to $\pi/2$, the rotor's crack is within the semi-open and the semi-closed state. Because the crack propagation applied to the crack's root to be caused by crack opening and closing is very small, the crack's opening and closing degree is considered to be 0. When it changes from 0 to $\pi/2$, the intermediate value φ will be processed with the cosine function. The model of the crack's opening and closing degree is shown as follows.

$$p=\tau\cos(\varphi). \quad (6)$$

When the angle φ continues to increase, the crack changes from the semi-open and the semi-closed state to the fully closed state.

2 HILBERT-HUANG MARGINAL SPECTRUM

Under the transient response of a rotor system, the vibration signals of a nonlinear cracked rotor show the non-periodic change and nonlinearity. Because the weak fault characteristic is easily hidden in other transitional components, the fault characteristic of a crack is difficult to extract from the vibration signals. The HHMS method is proposed to process the complex non-periodic and transient vibration signals. The frequency components in the signals of the transient response can be decomposed, and the fault characteristic can be extracted from the complex vibration signals by using the HHMS method.

2.1 Empirical Mode Decomposition

The complex non-stationary signal $x(t)$ can be represented a sum form of the intrinsic modal function (IMF) c_i and a residual component r_n by using the empirical mode decomposition (EMD) [7] and [21].

2.2 Hilbert Spectrum

After using the EMD, the Hilbert transform (HT) is used to compute each IMFs The computed equation is as follows.

$$y(t) = \frac{1}{\pi} p\int_{-\infty}^{+\infty} \frac{c(\tau)}{t-\tau} d\tau. \tag{7}$$

Through the HT processing, the analytical signal can be reconstructed. The expression is shown as follows.

$$z(t) = c(t) + jy(t) = a(t)e^{j\theta(t)}, \tag{8}$$

where $a(t) = (c^2 + y^2)^{1/2}$ and $\theta(t) = \tan^{-1}(y/c)$.

Where the instantaneous frequency and amplitude of each IMFs can be obtained, so the original signal can be expressed as follows.

$$x(t) = \mathrm{Re}\sum_{i=1}^{n} a_i(t)\mathrm{e}^{i\int \omega_i(t)dt}. \tag{9}$$

Because $\omega_i(t)$ is the instantaneous frequency, the residual function can be omitted. The Hilbert spectrum can be computed to use the following equation.

$$H(\omega, t) = \mathrm{Re}\sum_{i=1}^{n} a_i(t)\mathrm{e}^{i\int \omega_i(t)dt}. \tag{10}$$

Some information can be seen from the above equation. The $a_i(t)$ and $\omega_i(t)$ are functions of time variables and can form the three-dimensional spectrum picture with the time, the frequency and the amplitude.

2.3 Marginal Spectrum

The marginal spectrum [22] can be obtained by integrating the Hilbert spectrum along the time variable, and the computational expression is shown below.

$$h(\omega) = \int_0^T H(\omega, t)dt. \tag{11}$$

The marginal spectrum is the sum of the amplitude (energy) of a certain frequency in the signal, and it can also be understood that the sum of the amplitude of the frequency can be computed when the frequency appears at the whole processing. The frequency does not necessarily occur at the whole-time domain and does not necessarily only occur at a certain time. It may appear at several times with the different or same amplitude. The marginal spectrum realizes the distribution of the total amplitude for all frequencies in the signal, and it can accurately reflect the actual frequency components in the signal.

3 NUMERICAL SIMULATION

The effectiveness of the proposed HHMS method for the nonlinear cracked rotor system is investigated with numerical simulation. Using Eq. (4), the transient response of the cracked rotor is obtained based on the Runge-kutta method. The response curves can be calculated by using Eq. (7) to Eq. (11). The computational parameters are as follows. Obtaining suitable values $c=0.1$ and $\mathrm{e}=0.1$, the angle between crack direction and the eccentric $\beta=0$, the symmetric nonlinear coefficient $\beta^{(0)}=0.1$ and the asymmetric nonlinear coefficient $\varepsilon_c^{(1)}=\varepsilon_s^{(1)}=0.1$. The resonance curves and the crack's opening and closing degree are discussed with the influence of different rotor parameters.

3.1 Crack Detection Based on Transient Response

The transitional vibration signals of a rotor with a crack about five per cent of the depth [16] and [23] of the rotor's diameter are simulated and analysed using the wavelet method and the HHMS method, respectively. The simulation results of the two methods are compared with each other. There is only the major

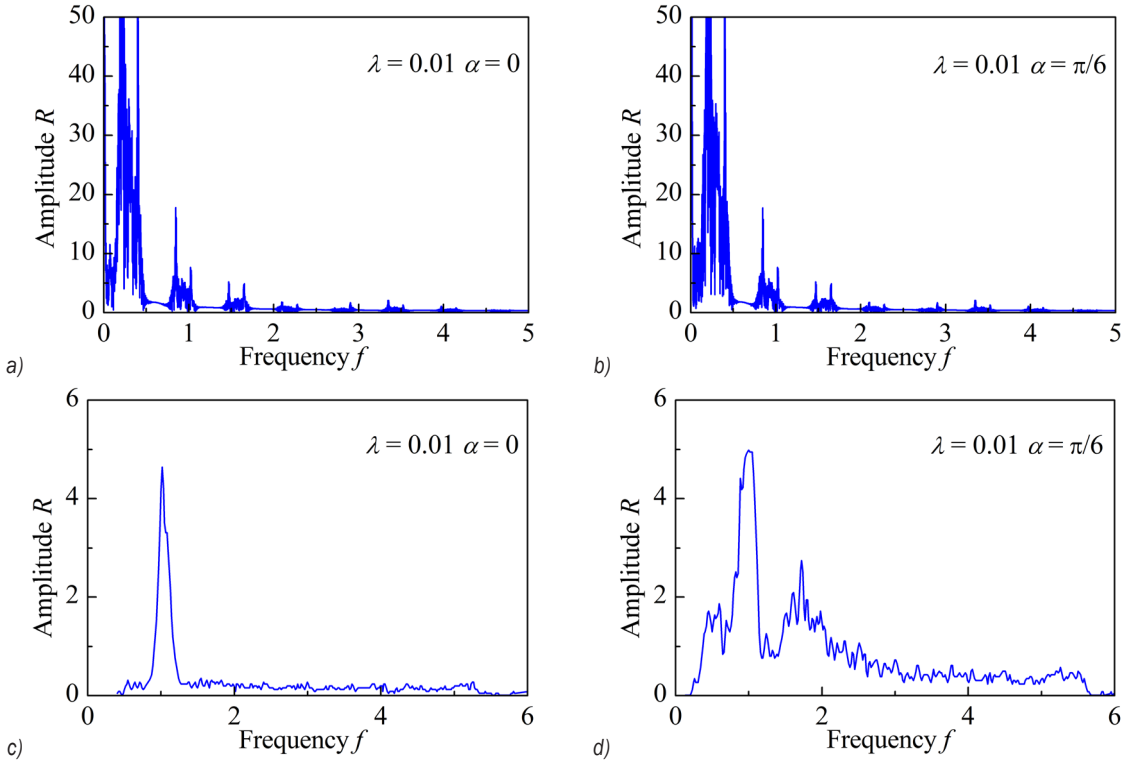

Fig. 4. *Simulation results; a) and b) using wavelet method; c) and d) using HHMS method*

harmonic vibration component in the spectrum of the normal rotor. However, there is not only the major harmonic vibration component, but also the super harmonic vibration component in the spectrum of the cracked rotor. The vibration component of the super harmonic can be used to determine the existence of a crack in a rotor system. The simulation results are shown in Figs. 4 and 5 based on the different rotational accelerations and crack angles. The abscissa is the vibration frequency component and the ordinate is the amplitude R.

3.1.1 Wavelet Method

Figs. 4a and b are the spectrum pictures of a normal rotor and a crack angle $\alpha=\pi/6$ under the rotational acceleration $\lambda=0.01$ to be calculated by the wavelet method. When the rotor does not have a crack, the calculation result is shown in Fig. 4a. There is the major harmonic vibration component, the sub-harmonic of order 1/2 vibration component, and the super-harmonic vibration component. When the rotor appears a crack and the crack angle $\alpha=\pi/6$, the calculation result is shown in Fig. 4b. The vibration components in the figure are similar to the result shown in Fig. 4a, and the corresponding amplitude does not change greatly. At each harmonic resonance, some clutter components exist, which are easily ignored. A misjudgment, whether the rotor has a crack or not, is easy to be made from above results by computing with the wavelet method.

3.1.2 HHMS Method

The analysis results with the HHMS method are shown in Figs. 4c and d. When the rotor does not have a crack, only the major harmonic vibration component exists, shown in Fig. 4c. When the rotor has a crack, and the crack angle $\alpha=\pi/6$, the corresponding calculation results shown in Fig. 4d under the rotational acceleration $\lambda=0.01$. There is the sub-harmonic of order 1/2 vibration component, the major harmonic vibration components and the super-harmonic vibration component to be caused by the existence of a crack. It can be seen that the results of the HHMS can be used to clearly determine whether the crack of the rotor system exists or not.

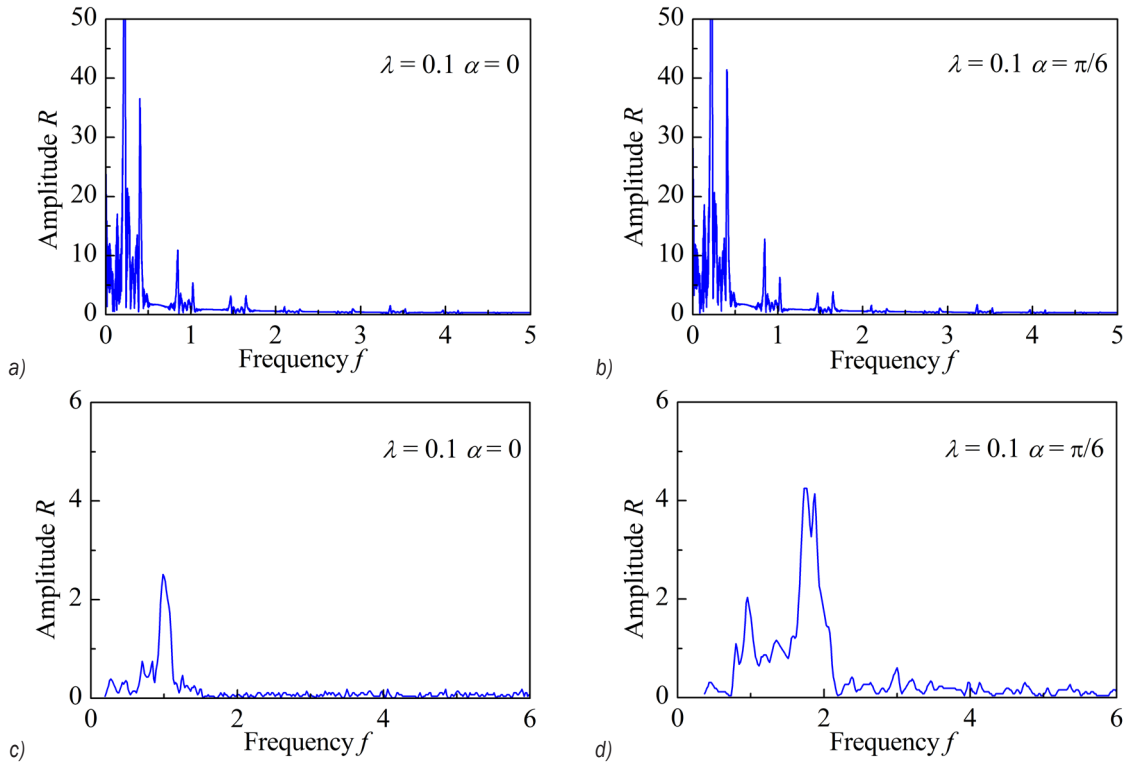

Fig. 5. *Simulation results; a) and b) using wavelet method; c) and d) using HHMS method*

3.1.3 Crack Detection Based on Acceleration Effect

Increasing the rotational acceleration λ to 0.1 and keeping other parameters unchanged, the calculation results are shown in Fig. 5 by using the wavelet method and the HHMS method, respectively. When the rotor does not have a crack, all the vibrational components are reduced by the wavelet method from comparing Fig. 5a with Fig. 4a. Comparing Fig. 5c with Fig. 4c to be computed by the HHMS method, the major harmonic vibration component is also reduced. However, the sub-harmonic of order 1/2 vibration component exists owing to the nonlinearity. When the rotor has a crack and the crack angle $\alpha=\pi/6$, the major harmonic vibration component is increased to compare Fig. 5b with Fig. 4b and the other vibration components are reduced. Comparing Fig. 5a with Fig. 5b, the vibration components are similar, and the amplitudes of components show little change. Therefore, changing the acceleration offers little help in detecting the rotor's crack with the wavelet method. Comparing the results shown in Fig. 5d with Fig. 4d, the major harmonic vibration component reduced due to the large rotational acceleration. However, the sub-harmonic of order 1/2 vibration component is almost reduced to zero, and the super harmonic vibration component increases remarkably. Therefore, increasing the rotational acceleration λ is beneficial to detect a crack with the HHMS method.

3.2 Delay Crack Propagation Based on Rotor Parameters Effect

Keeping the other rotor parameters unchanged, the crack's opening and closing degree is investigated by using the three types of rotor parameters. When the appropriate value of rotor parameters can reduce the crack's opening and closing degree, the delay crack propagation could be achieved. It is very important that we can adjust some parameter values to reduce the crack's opening and closing degree in an actual rotor system for the delay of crack propagation. The simulation results are shown in Fig. 6. The abscissa is time t, and the ordinate is the crack's opening and closing degree p.

3.2.1 Delay Crack Propagation Based on Acceleration Effect

The calculation results of the crack's opening and closing degree with different rotational accelerations λ are equal to 0.001, 0.01, and 0.1, and are shown in

Figs. 6a, b, and c. With the increase of the rotational acceleration λ, the crack's opening and closing degree decreases significantly. Its maximum value decreases from 0.027 shown in Fig. 6a to 0.016 shown in Fig. 6c, and the crack's opening and closing time is reduced from 1600 s to 100 s. The crack's opening and closing number reduces remarkably, shown in Figs 6a, b, and c. Therefore, when the rotor already has a crack, the acceleration value could appropriately increase under the transient running to reduce the crack's opening and closing degree to realize the delay of crack propagation.

3.2.2 Delay Crack Propagation Based on Angle β Effect

In [20], the influence of the angle β was discussed with the rotor vibration. This research has obtained a similar conclusion through simulation results. The crack's opening and closing degree is significantly reduced with the increase of the angle β. When the angle β changes to a small angle, the eccentric of the shaft is located in the same direction as the angle of the crack. The vibration amplitude of the rotor appears a large amplitude, so the crack's opening and closing degree is significantly increased. Therefore, when the rotor already has a crack, the delay of crack propagation could be achieved by adding a small mass on the disc to adjust the value of the angle β, shown in Fig. 2.

3.2.3 Delay Crack Propagation Based on Nonlinear Parameters Effect

The calculation results of the crack's opening and closing degrees with the value of the symmetric nonlinear parameter $\beta^{(0)}$, is equal to 0.05, 0.15, and 0.25, shown in Fig. 7. When the symmetric nonlinear parameter $\beta^{(0)}$ increases from 0.05 to 0.15, the corresponding crack's opening and closing degrees at the same time are reduced to some extent. When it increases from 0.15 to 0.25, the corresponding crack's opening and closing degree reduces at the forepart and increases at the rear part (t = 160 s later). The crack's opening and closing number significantly increases

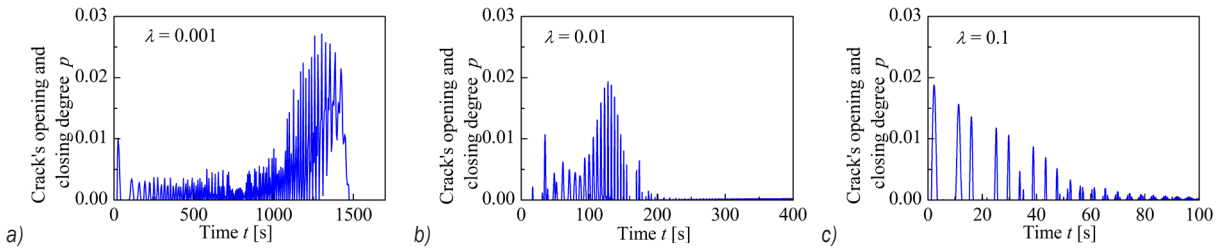

Fig. 6. *Crack's opening and closing degree with acceleration changing; a) λ = 0.001; b) λ = 0.01; and c) λ = 0.1*

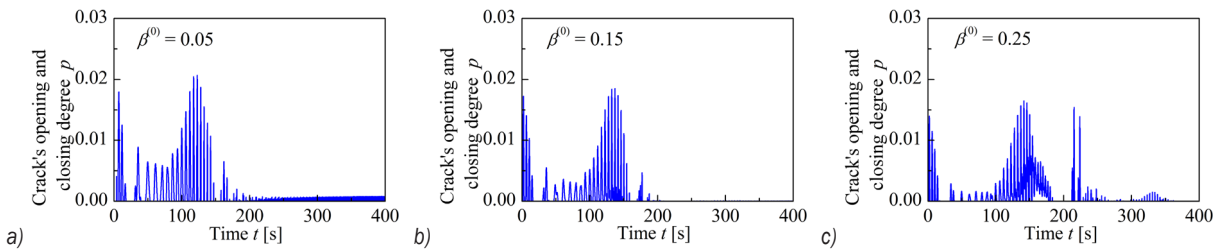

Fig. 7. *Crack's opening and closing degree with nonlinear parameter β(0) changing; a) β(0) = 0.05; b) β(0) = 0.15; and c) β(0) = 0.25*

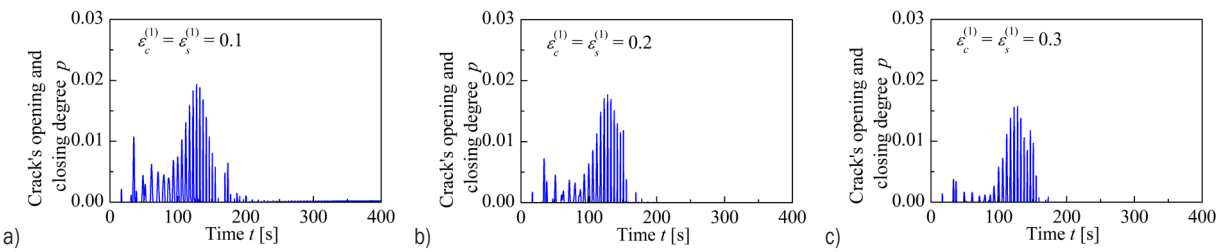

Fig. 8. *Crack's opening and closing degree with nonlinear parameters $\varepsilon_c^{(1)}$ and $\varepsilon_s^{(1)}$ changing; a) $\varepsilon_c^{(1)} = \varepsilon_s^{(1)} = 0.1$; b) $\varepsilon_c^{(1)} = \varepsilon_s^{(1)} = 0.2$; and c) $\varepsilon_c^{(1)} = \varepsilon_s^{(1)} = 0.3$*

from 140 s to 160 s; that is, a small $\beta^{(0)}$ is benefit to the delay crack propagation of a rotor system. Therefore, when a rotor already has a crack, the rotor support could be adjusted to decrease the value of the symmetric nonlinear parameter $\beta^{(0)}$ to realize the delay crack propagation.

The calculation results of the crack's opening and closing degree with the value of the asymmetric nonlinear parameters $\varepsilon_c^{(1)}$ and $\varepsilon_s^{(1)}$, are equal to 0.1, 0.2, and 0.3, and are shown in Fig. 8a, b, and c. The characteristics, seen from the figures, are that the crack's opening and closing degree corresponding to the same time is reduced and the crack's opening and closing number is also reduced with the increase of the asymmetric nonlinear parameters $\varepsilon_c^{(1)}$ and $\varepsilon_s^{(1)}$. Therefore, it can be concluded that we can adjust the rotor support to increase the value of the asymmetric nonlinear parameters $\varepsilon_c^{(1)}$ and $\varepsilon_s^{(1)}$ to realize the delay of crack propagation.

4 EXPERIMENT

4.1 Experimental Equipment

The experimental equipment is shown in Fig. 9. The disc is located on the centre of the elastic rotor, the left end of the rotor is supported by a self-aligning double-row ball bearing, and the right end is supported by a single-row deep-groove ball bearing. The length of the rotor is 505 mm; the diameter of the rotor is 10 mm. The disc diameter and thickness are 100 mm and 20 mm, respectively. The rotor with a crack is located to the left end of 290 mm, the crack length is 20 mm, and the depth is 1 mm. The crack is machined by the EDM machine, and the cut part was re-fixed into the rotor to form the crack. In the left side of the rotor sets the pulse encoder to detect the rotor rotational speed, its displacements in x- and y- directions are measured with the position sensor that were set at the right side of the disc. The experimental data is collected by computer and the Donghua software, the initial position is set at the rotational speed ω = 300 rpm.

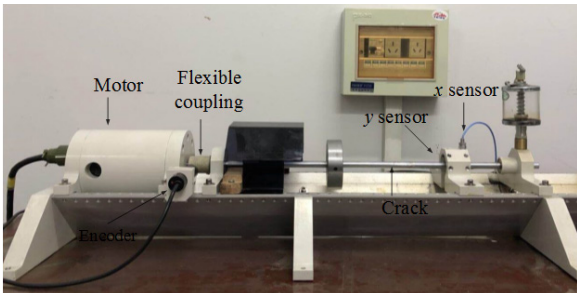

Fig. 9. *Experimental setup*

4.2 Experimental Result

4.2.1 Without Crack on the Rotor

First, the experiment was carried out by using a normal rotor. The rotational acceleration was set to 500 rpm/min and the experimental range was set from the rotational speed of 300 rpm to the rotational speed of 2000 rpm. The experimental resonance curves were tested by the above setup and processed by using the wavelet and the HHMS method. The experimental results are shown in Fig. 10. The vibration component of the rotor system is mainly 150 Hz. The vibration characteristics were lost to use the wavelet method shown in Fig. 10a. The experimental results show that the HHMS method is the better extraction than the wavelet method on the transient response.

4.2.2 Cracked Rotor

The experiment was carried by using the above-mentioned cracked rotor with a rotational acceleration λ = 500 rpm/min and the experimental range set from

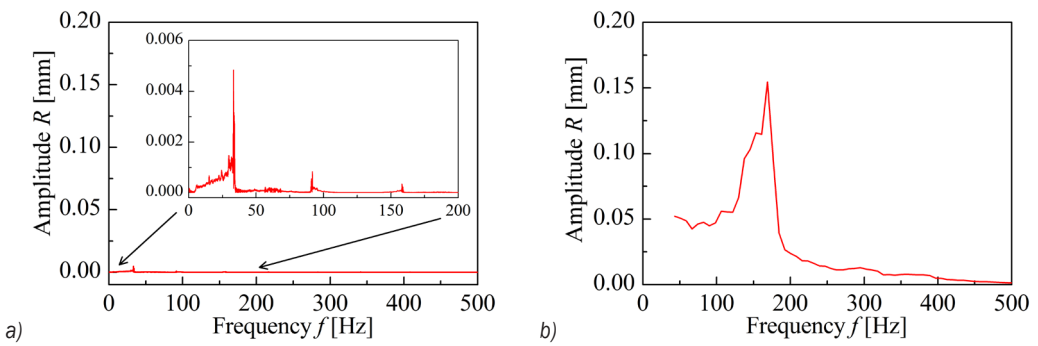

Fig. 10. *Experimental result without a crack; a) using wavelet method; and b) using HHMS method*

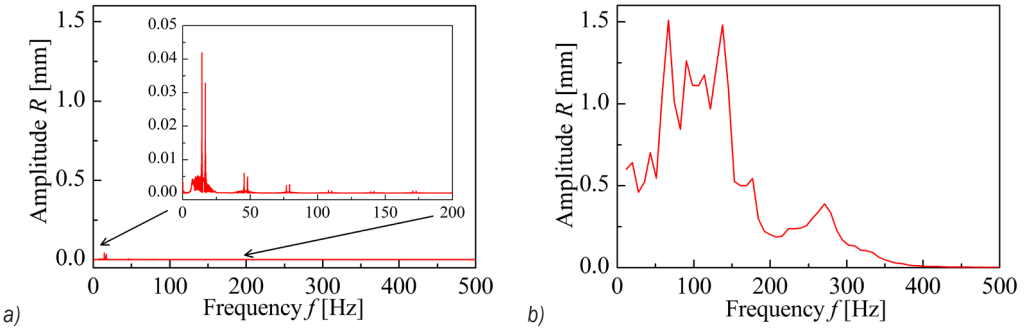

Fig. 11. *Experimental result with a crack; a) using wavelet method; and b) using HHMS method*

the rotational speed of 300 rpm to the rotational speed of 2000 rpm. The experimental resonance curves were also processed by using the wavelet and the HHMS method. The experimental results are shown in Fig. 11. The vibration components of the rotor system mainly have 150 Hz, 75 Hz and 100 Hz, respectively. In particular, the super harmonic vibration component is clearly revealed at 75 Hz, because the crack exists in the rotor system. In addition, the sub-harmonic of order 1/2 vibration component also appeared at the rotational position of 280 Hz due to the nonlinearity shown in Fig. 11b. Experimental results showed that the HHMS method is very effective for the fault detection of the transient rotor system.

5 CONCLUSIONS

In this research, the HHMS method is proposed for detecting a crack within the nonlinear rotor under the transient response. The simulation results show that it can effectively judge the existence of the early crack in a rotor system, and the crack which has about five percent of the depth of the rotor's diameter can be clearly judged by using HHMS. The experimental results also verify the effectiveness of the proposed HHMS method for the crack fault extraction from the transient response. This paper also proposes a novel method of describing the crack's opening and closing degree and discusses the delaying crack propagation with the different rotor parameters. The research results are proposed as follows.

1. The experimental and simulation results verify the effectiveness of the proposed HHMS method for the crack's fault extraction from the transient response, and the HHMS can accurately reflect the actual frequency components in the transient signal because of its integral effect.
2. When the aircraft takes off or landings, performs stunts, or makes a climbing-diving flight, the delay crack propagation can be achieved by increasing the rotational acceleration and deceleration.
3. When the angle β and the support of the rotor are adjusted effectively, the delay crack propagation can be achieved, such as reducing the symmetric nonlinear term $\beta^{(0)}$ and increasing the value of the asymmetric nonlinear term $\varepsilon_c^{(1)}$ and $\varepsilon_s^{(1)}$.

6 ACKNOWLEDGEMENTS

This work is supported by the Tianjin Natural Science Foundation of China (17JCZDJC38500 and 17JCYBJC18800) and the National Key Research and Development Program of China (2017YFB1303304).

7 NOMENCLATURES

a	depth of a crack, [m]
c	damping coefficient, [N·s·m^{-1}]
c_i	intrinsic modal function, [m]
e	static unbalance of the disk, [m]
h	thickness of the disk, [m]
k	stiffness coefficients, [N·m^{-1}]
l	length of a rotor, [m]
m	mass of disc, [kg]
N_x, N_y	nonlinear elastic restoring forces, [N]
r_n	residual component, [m]
x, y	displacements in x- and y-axis directions, [m]
$x(t)$	complex non-stationary signal, [m]
α	one-half angle of the crack [rad]
β	the angle between crack direction and the eccentric [rad]
$\beta^{(0)}$	symmetric nonlinear coefficient, [-]
δ	dimensionless factor, [-]
$\varepsilon_c^{(1)}$, $\varepsilon_s^{(1)}$	asymmetric nonlinear coefficient, [-]
θ	inclination angle, [rad]

λ rotational acceleration, [rad·s–2]
f_0 initial phase angle, [rad]
ω rotational speed, [rad·s–1]

8 REFERENCES

[1] Koc, A., Bartan, B., Gundogdu, E., Cukur, T., Ozaktas, H.M. (2017). Sparse representation of two-and three-dimensional images with fractional Fourier, Hartley, linear canonical, and Haar wavelet transforms. *Expert Systems with Applications*, vol. 77, p. 247-255, **DOI:10.1016/j.eswa.2017.01.046**.

[2] Yao, J., Tang, B., Zhao, J. (2016). Improved discrete Fourier transform algorithm for harmonic analysis of rotor system. *Measurement*, vol. 83, p. 57-71, **DOI:10.1016/j.measurement.2016.01.028**.

[3] Chandra, N.H., Sekhar, A.S. (2016). Fault detection in rotor bearing systems using time frequency techniques. *Mechanical Systems and Signal Processing*, vol. 72-73, p. 105-133, **DOI:10.1016/j.ymssp.2015.11.013**.

[4] Bashar, S.K., Bhuiyan, M.I.H. (2016). Classification of motor imagery movements using multivariate empirical mode decomposition and short time Fourier transform based hybrid method. *Engineering Science and Technology, an International Journal*, vol. 19, no. 3, p. 1457-1464, **DOI:10.1016/j.jestch.2016.04.009**.

[5] Dash, S.K., Rao, G.S. (2016). Arrhythmia Detection Using Wigner-Ville Distribution Based Neural Network. *Procedia Computer Science*, vol. 85, p. 806-811, **DOI:10.1016/j.procs.2016.05.269**.

[6] Cai, C.L., Xiong, H.L., Ling, Y. (2008). Blind processing method for frequency hopping signals based on Winger-Ville rearrangement and stationary wavelet. *Journal of Dalian Maritime University*, vol. 34, no. 4, p. 115-118.

[7] Wang, Y., Markert, R., Xiang, J., Zheng, W. (2015). Research on variational mode decomposition and its application in detecting rub-impact fault of the rotor system. *Mechanical Systems and Signal Processing*, vol. 60-61, p. 243-251, **DOI:10.1016/j.ymssp.2015.02.020**.

[8] Ren, Z., Zhou, S., E, C., Gong, M., Li, B., Wen, B. (2015). Crack fault diagnosis of rotor systems using wavelet transforms. *Computers & Electrical Engineering*, vol. 45, p. 33-41, **DOI:10.1016/j.compeleceng.2015.04.010**.

[9] Wang, D., Tsui, K.-L. (2017). Dynamic Bayesian wavelet transform: New methodology for extraction of repetitive transients. *Mechanical Systems and Signal Processing*, vol. 88, p. 137-144, **DOI:10.1016/j.ymssp.2016.11.003**.

[10] Huang, Q., Jiang, D., Hong, L. (2009). Application of Hilbert-Huang transform method on fault diagnosis for wind turbine rotor. *Key Engineering Materials*, vol. 413-414, p. 159-166, **DOI:10.4028/www.scientific.net/KEM.413-414.159**.

[11] Yan, J., Lu, L. (2014). Improved Hilbert-Huang transform based weak signal detection methodology and its application on incipient fault diagnosis and ECG signal analysis. *Signal Processing*, vol. 98, no. 4, p. 74-87, **DOI:10.1016/j.sigpro.2013.11.012**.

[12] Li, H., Zhang, Y., Zheng, H. (2009). Hilbert-Huang transform and marginal spectrum for detection and diagnosis of localized defects in roller bearings. *Journal of Mechanical Science and Technology*, vol. 23, no. 2, p. 291-301, **DOI:10.1007/s12206-008-1110-5**.

[13] Wang, C., Lu, J. (2010). Fault diagnosis of diesel engine based on HHT marginal spectrum. *Journal of Vibration Measurement & Diagnosis*, vol. 34, p. 1265-1272.

[14] Fu, K., Qu, J., Chai, Y., Zou, T. (2015). Hilbert marginal spectrum analysis for automatic seizure detection in EEG signals. *Biomedical Signal Processing & Control*, vol. 18, p. 179-185, **DOI:10.1016/j.bspc.2015.01.002**.

[15] Hou, L., Chen, Y., Lu, Z., Li, Z. (2015). Bifurcation analysis for 2:1 and 3:1 super-harmonic resonances of an aircraft cracked rotor system due to maneuver load. *Nonlinear Dynamics*, vol. 81, no. 1-2, p. 531-547, **DOI:10.1007/s11071-015-2009-1**.

[16] Ishida, Y., Yamamoto, T. (2013). *Linear and Nonlinear Rotordynamics: A Modern Treatment with Applications*. Wiley-VCH.

[17] Lu, Z., Hou, L., Chen, Y., Sun, C. (2016). Nonlinear response analysis for a dual-rotor system with a breathing transverse crack in the hollow shaft. *Nonlinear Dynamics*, vol. 83, no. 1-2, p. 169-185, **DOI:10.1007/s11071-015-2317-5**.

[18] Cavalini, A.A.Jr., Sanches, L., Bachschmid, N., Steffen, V.Jr. (2016). Crack identification for rotating machines based on a nonlinear approach. *Mechanical Systems and Signal Processing*, vol. 79, p. 72-85, **DOI:10.1016/j.ymssp.2016.02.041**.

[19] Wang, Z., Lin, W., Wen, B. (2010). Analysis on the stiffness of the rotor system with a switching crack. *Journal of Vibration and Shock*, vol. 29, no. 9, p. 69-72.

[20] Liu, J., Fan, Y., Wang, L.F., Chen, J., Wang, X., Liu, Z. (2016). Research of the delaying crack propagation on an aero-engine rotor. *International Journal of Mechatronics & Automation*, vol. 5, no. 4, p. 190-200, **DOI:10.1504/IJMA.2016.084217**.

[21] Lei, Y., Lin, J., He, Z., Zuo, M.J. (2013). A review on empirical mode decomposition in fault diagnosis of rotating machinery. *Mechanical Systems and Signal Processing*, vol. 35, no. 1-2, p. 108-126, **DOI:10.1016/j.ymssp.2012.09.015**.

[22] Huang, N.E., Shen, Z., Long, S.R., Wu, M.C., Shih, H.H., Zheng, Q., Yen, N.C., Chi, C.T., Liu, H.H. (1998). The empirical mode decomposition and the Hilbert spectrum for nonlinear and non-stationary time series analysis. *Proceedings Mathematical Physical & Engineering Sciences*, vol. 454, no. 1971, p. 903-995, **DOI:10.1098/rspa.1998.0193**.

[23] Ishida, Y. (2008). Cracked rotors: Industrial machine case histories and nonlinear effects shown by simple Jeffcott rotor. *Mechanical Systems & Signal Processing*, vol. 22, no. 4, p. 805-817, **DOI:10.1016/j.ymssp.2007.11.005**.